Journal of
Chemical Engineering & Process Technology

Reyes et al., J Chem Eng Process Technol 2014, 5:4
DOI; 10.4172/2157-7048.1000196

Research Article | Open Access

Tomato Dehydration in a Hybrid-Solar Dryer

Reyes A*, Mahn A, Huenulaf P and González T

Department of Chemical Engineering, University of Santiago of Chile, Av. L. B. O"Higgins 3363, Santiago, Chile

Abstract

Tomato pieces were dehydrated in a hybrid solar dryer provided with a 3 m^2 solar panel and electric resistances. At the outlet of the tray dryer 80 or 90% of the air was recycled and the air temperature was adjusted 50 or 60ºC. At the outlet of the solar panel the air temperature raised between 5 and 18°C above the ambient temperature.

Temperature and sample size significantly affected critical moisture content. The color parameters of dehydrated tomato indicate a notorious redness. Rehydration was achieved in less than 50 minutes.

Drying kinetics was adequately adjusted with three empirical models. Sorption isotherms adjusted soundly well with the Guggenheim-Anderson-de Boer and Peleg models. The solar energy input resulted in 6.6-12.5% energy saving.

Keywords: Drying; Solar energy; Hybrid solar dryer; Tomato; Water activity

Nomenclature

a: Activity

a*: Colour parameter

Ap: Solar panel area m^2

b: Parameter s/m

b*: Colour parameter

c: Dimensionless parameter

C: Peleg parameters

E: Colour parameter

K: Page parameter

I: Solar radiation W/m^2

L*: Colour parameter

Mo: Initial moisture content on dry basis Kg/kg

Mw: Moisture content on dry basis Kg/kg

n: Page parameter

N: Number of experimental data

Qe: Electric energy input Joule

Qsp: Absorbed solar energy Joule

R: Air recycle %

RH: Relative air humidity

RMSE: Root mean squared error

T: Drying air temperature °C, K

t: Time:minutes

v: Air velocity, inside the chamber m/s

X: Average moisture content of tomato particles water kg/kg wb

Xo: Initial moisture content of tomato particles water kg/kg wb

Xeq: Equilibrium moisture content of tomato water kg/kg wb

Greek Letters

a: Tilt of the solar panel (a=11º)

Δ: Difference between two values

Sub-indexes

amb: ambient

c: critical

o: initial

sp: solar panel outlet

eq: equilibrium

w: water

Introduction

Drying is one of the most energy-intensive processes in the food industry [1-3]. For this reason, the partial (or total) replacement of traditional fuels by renewable sources of energy in drying processes will result in considerable energy savings. Additionally, solar energy is an attractive non-polluting alternative [1,4,5]. However, the daily and seasonal fluctuations in the irradiation level are some drawbacks that make it necessary to use additional energy sources that permit the operation during the low irradiation periods.

Chile is located in the southwest hemisphere, at the west from Greenwich meridian, between 17° 30' and 90° south latitude, with marked irradiation differences along the country. In this sense, the Metropolitan region, where the capital Santiago is found, exhibits an irradiation level similar to that of the central zone of Chile. In addition, energy consumption projections in Chile indicate a serious energy

***Corresponding author:** Reyes A, Department of Chemical Engineering, University of Santiago of Chile, Av. L. B. O"Higgins 3363, Santiago, Chile, Tel: 5627181833; E-mail: alejandro.reyes@usach.cl

Received May 05, 2014; **Accepted** May 31, 2014; **Published** June 02, 2014

Citation: Reyes A, Mahn A, Huenulaf P, González T (2014) Tomato Dehydration in a Hybrid-Solar Dryer. J Chem Eng Process Technol 5: 196. doi: 10.4172/2157-7048.1000196

deficit for the next decade, and therefore solar energy constitutes an interesting alternative.

The drying process involves simultaneous: (i) heat transfer from the surrounding to the surface of the food particle being dried followed by heat conduction within the material; and (ii) mass transfer from inside the food to its surface, followed by external transport of moisture to the surroundings. The heat is transferred to the surface of food particle by conduction and convection from adjacent air at temperature above that of the material being dried. The drying air absorbs moisture from the solid only if its relative humidity is below saturation [6].

In indirect solar drying, the foodstuff is kept inside a drying chamber, in which the pre-heated air from the flat plate collectors enters. In order to allow using the solar dryer in low or null irradiation periods, hybrid solar dryers that consider the use of additional energy sources (biomass, hydrocarbons or electricity) have been developed [7-10].

Flat plate collectors consist of: (1) a dark flat-plate absorber of solar energy, (2) a transparent cover that allows solar energy to pass through, (3) a space through which drying air flows, and (4) a heat insulation lower base [2,11,12]. The use of roughness elements or porous matrixes acting as absorber has been used as an alternative to improve heat transfer.

Several experimental works related with fruit and vegetables dehydration in hybrid solar dryers that use electric or biomass supplementary energy have been reported [6,9,13-25].

There are phenomenological models based on the second Fick's law, which use different approaches, to describe the drying process [26]. Besides, there are several empirical models which are useful when the solid has a heterogeneous composition (skin, seeds, pomace, etc.), geometry is difficult to characterize and/or changes dramatically during the drying process. The main similarity of most empirical models is the exponential term. Among these models are found the Page model [27], given by Eq. 1, the modified Page model [28], given by Eq.2, and the Henderson and Pabis model [29], given by Eq. 3.

$$\frac{X(t)}{X_0} = exp(-k \cdot t^n) \tag{1}$$

$$\frac{X(t)}{X_0} = exp(-k \cdot t)^n \tag{2}$$

$$\frac{X(t)}{X_0} = aexp(-k \cdot t) \tag{3}$$

Water activity (i.e. the ratio of the vapor pressure in a food material to that for pure water at the same temperature) is related with the equilibrium moisture content through a water sorption isotherm, at constant temperature. The water sorption isotherms of most foods are nonlinear, exhibiting a sigmoid shape. Isotherms are obtained by exposing a small sample of food to different constant relative humidity atmospheres. Once reached equilibrium, the water content of the sample is determined gravimetrically. In many cases, the process of sorbing or desorbing water may change the solid matrix and consequently affect the sorption behavior, thus triggering the hysteresis phenomena [30]. One of the most relevant equations used to represent sorption data is the Guggenheim-Anderson-de Boer (GAB), given by Eq. 4, which is reported to be the best for fitting sorption isotherm data for the majority of food products up to a_w levels of approximately 0.9 [31].

$$M_w = \frac{M_o \cdot C \cdot K \cdot a_w}{(1 - K \cdot a_w)(1 - K \cdot a_w + C \cdot K \cdot a_w)} \tag{4}$$

Another one, the Peleg model (1993) [32], has four parameters and is given in Equation. 5:

$$M_w = C_1 \cdot a_w^{C_3} + C_2 \cdot a_w^{C_4} \tag{5}$$

where C_1, C_2, C_3 and C_4 are constants.

Tomato (*Lycopersicom esculentum*) is the world's most commercially produced vegetable [33]. It is a rich source of minerals, vitamins, organic acid, and dietary fiber [34], and therefore its consumption has been intensified in different presentations: fresh, juice, puree, canned, and dressings. Tomato has a high content of lycopene, ascorbic acid and flavonoids, which offer important healthy effects [33-35].

Currently more than 20 000 tomato cultivars are known worldwide, which differ in size, color, shape, flavor and chemical composition.

Considering that tomato production is markedly seasonal, a preservation alternative is dehydration, in order to increase its availability. Dried tomatoes have become a highly attractive product and their demand has increased significantly during the last years [35-37].

The purpose of the present work was to analyze the drying of tomatoes (plum tomato) using a hybrid solar dryer, the determination of water activity and some quality parameters.

Material and Methods

Equipment

The hybrid solar dryer (HSD) consists of a 3 m^2 (3 m length and 1 m width) solar panel composed by a glass sheet cover (5 mm thickness) and a black wavy zinc plate. Below this zinc plate a thermal insulating material was inserted (50 mm thickness). The air passes through the free space (30 to 50 mm height) between the glass and the zinc plate until reaching the mixing point with the recycled air. This air mixture enters the electric heating system composed by 5 kW electric resistances where the air temperature is adjusted to the desired level (50 or 60°C). After that, the air enters the drying chamber (0.5 m*0.5m *1.2 m), where it distributes to pass over 10 perforated plate trays made of stainless steel (0.45m*0.5m), located in two sections of 5 trays each one.

The air is sucked through a 3 kW blower and directed to the electric resistances zone, although a 10-20 % fraction is removed from the system through valve V_2.

The HSD is provided with a data acquisition system OPTO 22 (model SNAP-PAC-R1), which allows registering air temperature at the outlet of the solar panel (Ts), temperature and relative humidity in the drying chamber, just before the inlet of the drying chamber (T_1 and RH_1) [Hanna Instruments, HI 8666, RH/ºC s] and temperature and relative humidity in the drying chamber immediately before the outlet (T_2 and RH_2). Air flow rate was determined by the pressure drop registered through two Pitot tubes located at the outlet of the centrifugal fan and the outlet of valve V_2. The solar radiation was determined by a Pyranometer (LI-200SA) located at one side of the solar panel. This information was stored in a PC. The solar panel was located on the roof of a four-floor building corresponding to Unit Operation Laboratory of the Department of Chemical Engineering. The drying chamber and the control system were installed in the 4th floor, just below the solar panel. Air passage valves opening was controlled from a PC.

Citation: Reyes A, Mahn A, Huenulaf P, González T (2014) Tomato Dehydration in a Hybrid-Solar Dryer. J Chem Eng Process Technol 5: 196. doi: 10.4172/2157-7048.1000196

Materials

Drying runs were performed using plum tomatoes, purchased at the local market, characterized by an oval shape, intense red color. The tomatoes were manually chosen, having average dimensions of 4.0 ± 0.3 cm diameter and 9.0 ± 0.3 cm length, measured with a Vernier calipter. After that, tomatoes were thoroughly rinsed. Then, tomatoes were cut longitudinally in quarters or eighths. This was necessary because the tomatoes skin represents a barrier to moisture removal, and a higher exposure of the tomatoes flesh improves water diffusion, thus shortening the drying process. Additionally, substrate size must take into account the expectations of consumers.

Experimental designs

Selection of the experimental factors considered initial tomato size (1/4 and 1/8) because it affects the diffusion path of moisture; air flow recycle (80 and 90%) since this implies minimizing energy supply to heat the drying air, and drying air temperature (50 and 60°C). The temperature levels were chosen based on the fact that temperatures lower than 50°C result in an excessively slow drying process, and temperatures above 60°C may impair the product quality. A factorial experimental design, with the above-mentioned factors in two levels (2^3), was used to analyze the drying process. Table 1 shows the experimental design matrix. Runs were carried out in a random order.

Statistical analyses

The experimental data obtained from the execution of the experimental design (Table 1) were analyzed through ANOVA (at 95% confidence), and the statistical effect of the experimental factors on moisture content were calculated at different points during the drying process, and their significance was determined. A statistical effect represents the magnitude of the change in the response variable when a factor passes from the low level to the high level. The analyses were performed with Statgraphics Centurion.

Run	Air Recycle (%)	Temperature [ºC]	Fraction pieces
T1	90	50	1/8
T2	80	60	1/8
T3	80	50	1/4
T4	90	60	1/4
T5	90	60	1/8
T6	90	50	1/4
T7	80	50	1/8
T8	80	60	1/4

Table 1: Experimental design matrix.

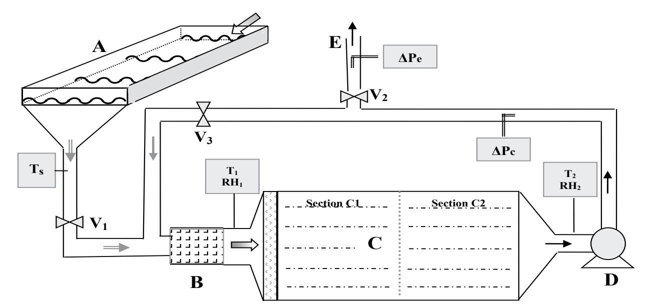

Figure 1: Hybrid-solar dryer. A. Solar panel; B. Electrical heater; C. Chamber drying; D. Centrifugal fan; E. Exit air. V_i. Valves.

Drying procedure

About 6.5 kg of tomato pieces were put in the dryer, distributing 0.650 kg in each tray (0.48 m * 0.58 m). Additionally 0.050 kg was loaded in two wire baskets, which were located in section 1 and 2, respectively. To obtain the drying curves, samples of the solids were removed from two sectors of the dryer, weighed on a digital balance with a sensitivity of 0.01 g (Boeco BBL62, Boecktel Co., Germany) and then put back in the dryer, and removed again every 30 minutes. The moisture content for each point of the drying curve was determined by calculating the difference in weight between the wet state and the dry weight after drying exhaustively at 85ºC.

Water activity measurement

Relative moisture content, necessary to obtain the sorption isotherms, was determined using Thermoconstanter Humidat TH-2 of Novasina. First, the equipment was calibrated using standardized salt solutions, as suggested by the manufacturer. The desorption isotherms were determined using dehydrated tomato samples in a laboratory tunnel dryer at 70°C and air flow rate of 2 m/s. During the dehydration process, samples were withdrawn at different drying times, and consequently showing different moisture content. Moisture content was determined in a vacuum oven until constant weight according to AOAC 920.151 (AOAC, 1990). The mean of three measurements (within ± 0.01 g) was reported. Approximately 5.0 g of partially dehydrated samples were placed into Petri dishes and then into Novasina Instrument. Isotherms were determined at 15, 25 and 40ºC.

Colour procedure

The colour of the samples was measured with a colorimeter (Minolta Chromo Meter CR 200b) using the L^* a^* b^* colour scale, which is an international standard for color measurements, adopted by the Commission Internationale d'Eclairage (CIE). The instrument was calibrated with white and yellow plates. Surface measurements were made under a CIE D_{65} illuminant which simulates diffused daylight. Colour measurements of tomatoes were made on a Petri dish over a white plate and replicated ten times after mixing the dried samples, and the average values of L^*, a^* and b^* were reported. Mixing of samples was done primarily to account for colour variation among dehydrated tomatoes particles.

Colour variation between fresh (denoted by the subscript 'o') and dehydrated tomatoes, was used to describe the total colour change ΔE after drying by means of Eq. 6 (http://www.cie.co.at/).

$$\Delta E = \sqrt{\left(L_0^* - L^*\right)^2 + \left(a_0^* - a^*\right)^2 + \left(b_0^* - b^*\right)^2} \tag{6}$$

Rehydration tests

The water adsorption capacity of the dried particles was determined in a water thermostatic bath at 35 ºC. 10 g of dried material were put in a wire basket and were immersed in a water bath. The basket was removed from the bath at different time intervals, the surface water was removed with an adsorbent paper and the total mass was determined. Then the basket was immersed in the bath again. The first five measurements were taken every two minutes, and after that, when the variation in mass was too low, a sample was taken every 5 minutes until 60 minutes. All measurements were made in triplicate (Figure 1).

Results and Discussion

Data acquisition

Ambient temperature, air temperature in the outlet of the solar

Citation: Reyes A, Mahn A, Huenulaf P, González T (2014) Tomato Dehydration in a Hybrid-Solar Dryer. J Chem Eng Process Technol 5: 196. doi: 10.4172/2157-7048.1000196

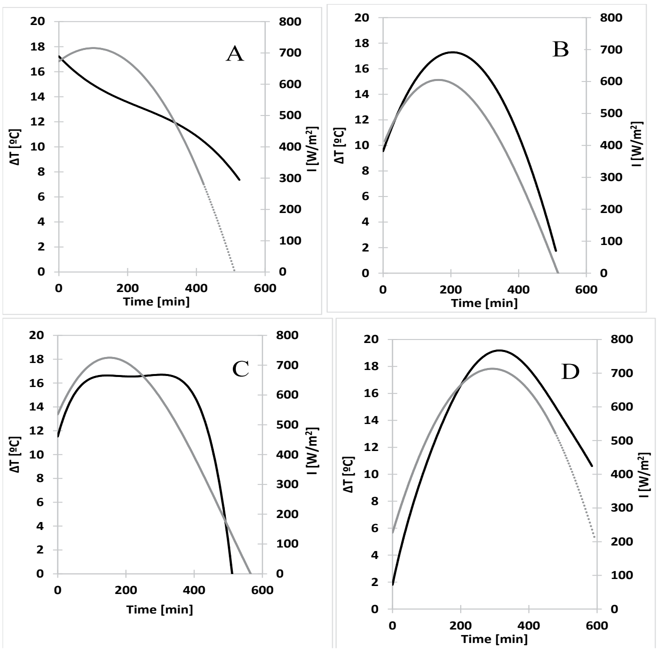

Figure 2: Solar radiation and ΔT (Solar panel temperature - Ambient temperature). A) Run T1, B) Run T2, C) Run T4 and D) Run T8. (-----Solar Radiation, ______ ΔT).

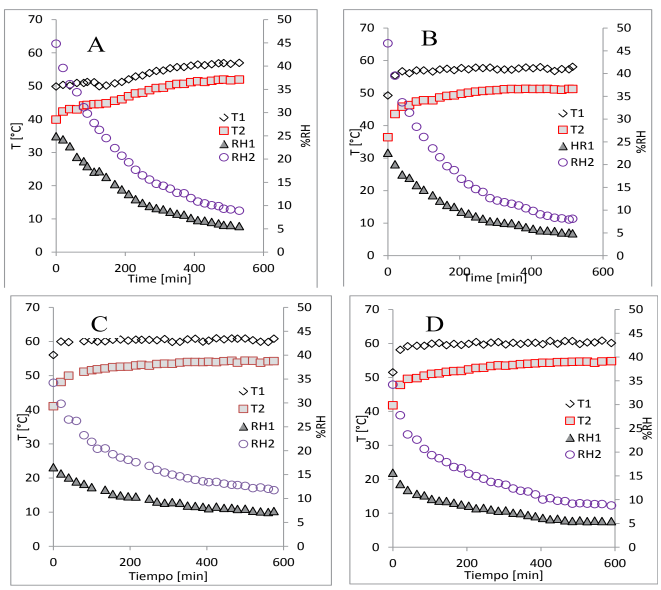

Figure 3: Temperature and relative humidity at the inlet and outlet of the drying chamber. (A) Run T1, (B) Run T2, (C) Run T4, and (D) Run T8.

panel (T_{sp}), and solar radiation were registered through the data acquisition system. This is shown in Figure 2 for runs T1, T2, T4, and T8. The ambient temperature fluctuated between 20ºC and 31ºC, depending on the day and time of the measurement. The solar panel allowed increasing the air temperature (T_{sp}) up to 18°C above the ambient temperature, depending on the air flow rate and mainly of the solar radiation. This temperature increase allows reducing electric energy consumption. The difference to achieve the pre-defined inlet air temperature (T_1) was obtained from the electric resistances.

Figure 2 shows that during the complete drying period, at least during 360 minutes the radiation level remained above 200 W/m^2, with maximum values higher than 600 W/m^2 for a period of 100-200 minutes period.

Air temperature (T_1 and T_2) and relative air humidity (RH_1 and RH_2) at the inlet and outlet of the drying chamber were also registered, which are presented for some runs in Figure 3.

Figure 3 shows that the air temperature at the inlet of the drying chamber kept at the pre-fixed value (50 or 60ºC) with variations of ± 2ºC. An exception was observed in run T1 (Figure 3A), where form the 200th minute on wards the temperature raised up to 57°C, despite the electric resistances were turned off, due to the specially high solar radiation during that day.

Figure 3 also shows that in the first 120-200 minutes the air temperature diminishes when passing through the drying chamber in about 12°C. By the end of the drying process this difference decreases to 6 °C, due to the lower remaining moisture content of the solids. The air that enters the drying chamber comes from the solar panel (fresh air) (10 or 20% of total air flow) and from the outlet of the dryer itself (recycled air) (80-90 % total air flow). For this reason the humidity of the air that enters the drying chamber varies during the drying process: ~30% humidity at the beginning of the process, and diminishing until ~10% by the end of the process. On the other hand, the relative humidity of the air at the outlet of the dryer, at the beginning of the process is in the order of 60 ± 5%, diminishing to 20% by the end of the process, as a consequence of the lower moisture content removed in the final drying period.

Experimental drying curves

Figure 4 shows the reduced drying curves (dimensionless moisture content v/s time), executed in duplicate, corresponding to runs carried out at operating conditions given in Table 1. The drying experiences were stopped when X/X0 reached 0.1 or after 600 minutes of drying because after that time the effect of solar radiation was negligible, independently from the final moisture content of the final product. In Figure 4, X_o represents the average initial moisture content (X_o=15.667 dry base). Overall the results showed deviations lower than 2 %. The drying curves exhibited the expected behavior: a linear decrease of moisture content in the initial period, until reaching the critical moisture content, where the non-bound moisture was removed; and after that the bound moisture was removed following an exponential trend in terms of time. Figure 4 shows that drying air temperature

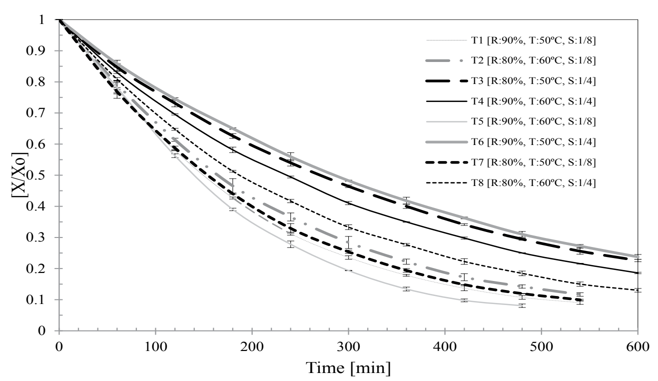

Figure 4: Drying kinetics of tomatoes (R: recycle, T: temperature, S: size).

Citation: Reyes A, Mahn A, Huenulaf P, González T (2014) Tomato Dehydration in a Hybrid-Solar Dryer. J Chem Eng Process Technol 5: 196. doi: 10.4172/2157-7048.1000196

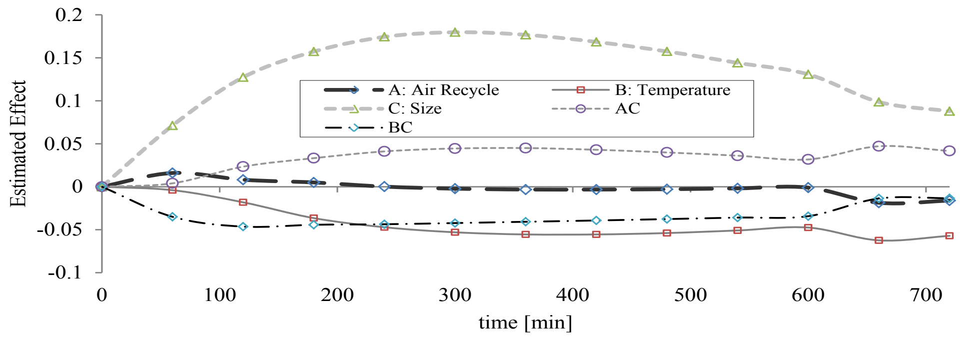

Figure 5: Evolution of significant effects on moisture content, at 95% confidence level.

	Page						Henderson and Pabis		
	k	n	R^2	k	n	R^2	k	n	R^2
T1	0.0033	1.1579	0.9993	0.0046	1.0089	0.9961	0.0047	1.0121	0.9965
T2	0.0028	1.1086	0.9974	0.0039	1.0667	0.9988	0.0042	1.0051	0.9989
T3	0.0035	1.1715	0.9986	0.0026	0.9726	0.9986	0.0025	0.9926	0.9988
T4	0.0047	1.1414	0.9962	0.0029	0.9860	0.9989	0.0029	0.9903	0.9992
T5	0.0014	1.2211	0.9986	0.0062	0.9184	0.9940	0.0053	1.0273	0.9954
T6	0.0017	1.1299	0.9987	0.0024	0.9897	0.9989	0.0024	0.9973	0.9991
T7	0.0023	1.1795	0.9996	0.0050	0.9221	0.9991	0.0045	1.0026	0.9991
T8	0.0056	1.1039	0.9976	0.0036	0.9756	0.9965	0.0036	0.9966	0.9992

Table 2: Page, modified Page and Henderson and Pabis models parameters with the corresponding R^2 values.

Run	X_c/X_o Block 1	X_c/X_o Block 2
T1	0.45	0.43
T2	0.43	0.48
T3	0.50	0.53
T4	0.59	0.55
T5	0.40	0.41
T6	0.54	0.51
T7	0.41	0.40
T8	0.59	0.60

Table 3: Values of X_c/X_o for tomatoes.

and sample size exhibited the expected behavior: higher temperatures resulted in faster drying kinetics and when diminishing the sample size, faster drying rates was observed, accounting for the reduction of the diffusional path. Air recycle had no significant effect probably due to its low variation imposed.

Figure 5 shows the evolution in time of the effects of the operational variables on moisture content during the drying process. From the 120th minute onwards a clear effect of sample size was observed, while air temperature begins to be statistically significant from the 200th minute onwards, agreeing with the end of the first drying stage. Air recycle had no statistical effect, but its interaction with sample size does.

Adjustment of experimental drying kinetics

Given that tomato particles showed an irregular shape, drying curves were adjusted only with the empirical models of Page [27], given by Eq. 1, the modified Page [28], given by Eq.2, and Henderson and Pabis [29], given by Eq. 3. This adjustment was performed by the Solver Tool from Microsoft Excel 2003 software, minimizing the root mean square error between the experimental values of moisture content of the tomatoes particles versus time and those calculated for the models. As shown in Table 2, the resulting R^2 values for three models were higher than 0.99, being slightly better the adjustments of Henderson and Pabis model.

Critical moisture content

In the plots of dX/dt versus X (data not shown), it was not possible to clearly visualize the change from the constant rate period to the falling rate period. For this reason, the critical moisture content (shown in Table 3) was obtained from the slope change in moisture content versus time plots. The procedure consisted in adjusting a straight line to the three initial points of each drying curve. Then, the line was extrapolated to the complete drying curve. The experimental points were compared with the corresponding points of the straight line, and the standard deviation was calculated. When standard deviation exceeded 0.035, we considered that at that point the straight line did not represent the constant rate period. Accordingly, this point corresponds to the critical moisture content.

Drying time decreased proportionally to X_c, since higher values of X_c result in shorter constant drying rate periods (highest drying rate). For this reason, and considering as unique criterion the minimization of the drying period, it is recommendable selecting operating conditions that reduce the critical moisture content. However, in the final decision

Citation: Reyes A, Mahn A, Huenulaf P, González T (2014) Tomato Dehydration in a Hybrid-Solar Dryer. J Chem Eng Process Technol 5: 196. doi: 10.4172/2157-7048.1000196

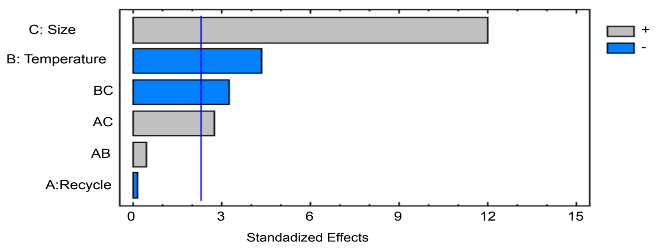

Figure 6: Pareto chart.

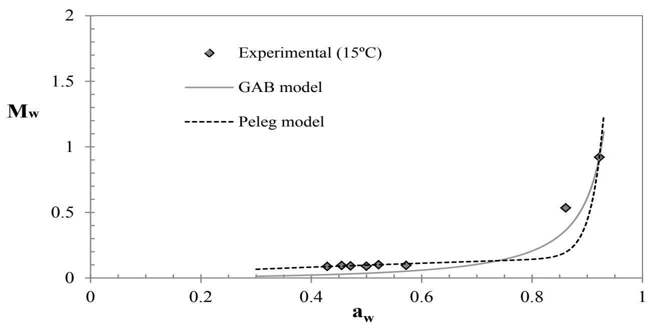

Figure 7: Desorption isotherm of tomatoes at 15°C.

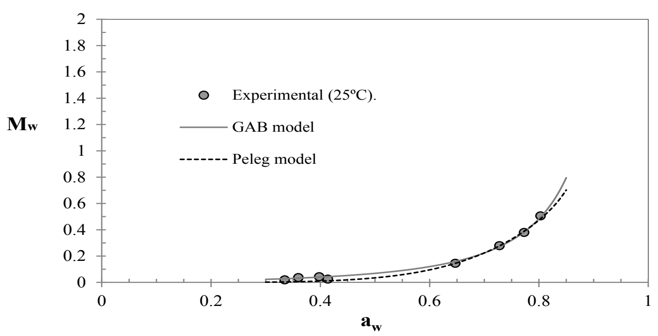

Figure 8: Desorption isotherm of tomatoes at 25 °C.

regarding the most adequate drying parameters, the effect of these parameters on product quality should also be considered.

The Pareto chart (Figure 6) shows that X_c diminished with temperature increase, and it increased with sample size, as well as the binary interactions. Air recycle did not affect X_c.

Water sorption isotherms

The desorption isotherms of tomato samples with different moisture content were determined at 15, 25 ad 40°C. Then the isotherms were adjusted with the Guggenheim-Anderson-Boer (GAB) (Eq. 4) and the Peleg model (Eq. 5). Both models offered a good adjustment quality, with RMSE lower than 0.25. Figures 7, 8 and 9 compare predictions from both models with the experimental data at 15, 25 and 40°C. Table 4 shows the parameters of both models for each temperature in the desorption process.

Color

The color parameters (a^*, b^*, ΔE, and L^*) of dehydrated tomatoes are given in Table 4. The statistical analysis of these parameters indicate that only a* is affected by the operational variables, with the air temperature showing the highest effect. The increase of a* confirms the intensification of redness in all runs (Table 5), with respect to fresh tomatoes. This effect increases directly with temperature. Redness variations was also reported by Kerkhofs et al. [37], and it was attributed to a combination of non-enzymatic browning, Maillard reaction and lycopene degradation.

Rehydration of the dried tomato particles

On checking the rate of rehydration of dried tomato particles, all experiments showed that this rate was high during the first 3 minutes of the rehydration procedure, and then it was followed by a period of asymptotic increase during the next 15 minutes, with not significant increases from this point onwards, as shown in Figure 10. The final water content after rehydration was 0.75 ± 0.05 for all runs. The time required to reach this moisture content was shorter for the thinnest slices due to the shorter diffusional path of water.

Adjustment of experimental drying kinetics

Drying curves were adjusted only with the empirical models of Page [27], given by Eq. 1, the modified Page [28], given by Eq.2, and Henderson and Pabis [29], given by Eq. 3. This adjustment was

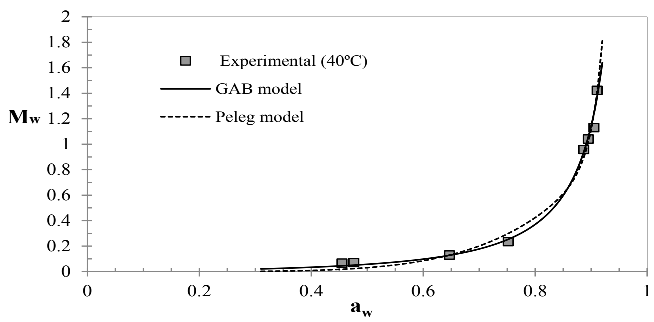

Figure 9: Desorption isotherm of tomatoes at 40 °C.

Model	Parameters	15ºC	25ºC	40ºC
GAB	Mo	0.053	0.178	0.118
	C	0.466	0.225	0.298
	K	1.028	1.020	1.023
	RMSE	0.24	0.08	0.17
Peleg	C_1	0.166	1.616	1.468
	C_2	20.154	28.907	52.607
	C_3	0.758	5.541	5.576
	C_4	40.275	39.704	48.931
	RMSE	0.20	0.11	0.20

Table 4: Peleg and GAB model parameters for isotherms of plum tomato.

Run	ΔE	ΔL	Δa*	Δb*
T1	19.66	11.07	2.77	15.90
T2	13.461	9.39	2.11	9.41
T3	16.681	9.79	7.11	11.49
T4	14.447	8.89	5.31	10.07
T5	18.678	10.85	5.06	14.34
T6	15.300	9.61	6.15	10.20
T7	15.973	9.64	4.73	11.83
T8	20.787	12.78	1.05	16.36

Table 5: Color parameters.

Citation: Reyes A, Mahn A, Huenulaf P, González T (2014) Tomato Dehydration in a Hybrid-Solar Dryer. J Chem Eng Process Technol 5: 196. doi: 10.4172/2157-7048.1000196

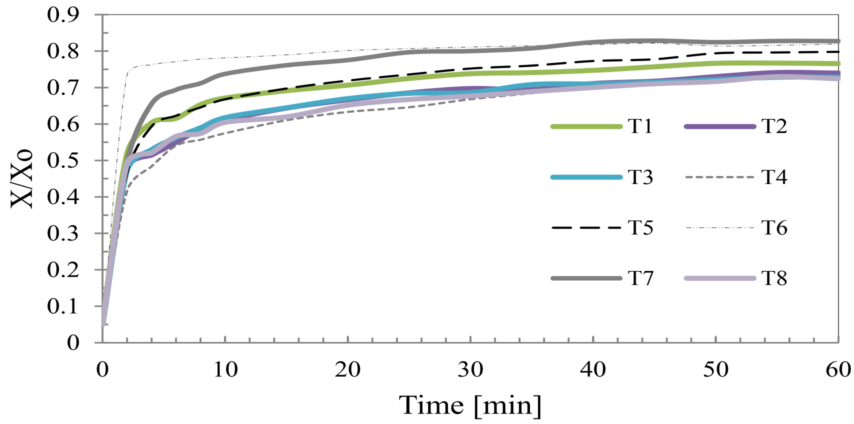

Figure 10: Rehydration profiles of tomato.

	Page						Henderson and Pabis		
	k	n	R^2	k	n	R^2	k	n	R^2
T1	0.0033	1.1579	0.9993	0.0046	1.0089	0.9961	0.0047	1.0121	0.9965
T2	0.0028	1.1086	0.9974	0.0039	1.0667	0.9988	0.0042	1.0051	0.9989
T3	0.0035	1.1715	0.9986	0.0026	0.9726	0.9986	0.0025	0.9926	0.9988
T4	0.0047	1.1414	0.9962	0.0029	0.9860	0.9989	0.0029	0.9903	0.9992
T5	0.0014	1.2211	0.9986	0.0062	0.9184	0.9940	0.0053	1.0273	0.9954
T6	0.0017	1.1299	0.9987	0.0024	0.9897	0.9989	0.0024	0.9973	0.9991
T7	0.0023	1.1795	0.9996	0.0050	0.9221	0.9991	0.0045	1.0026	0.9991
T8	0.0056	1.1039	0.9976	0.0036	0.9756	0.9965	0.0036	0.9966	0.9992

Table 6: Page, modified Page and Henderson and Pabis models parameters with the corresponding R^2 values.

Run	Average [Qsp/Qe]	Standard deviation
T1	0.100	0.010
T2	0.076	0.016
T3	0.082	0.034
T4	0.066	0.025
T5	0.079	0.010
T6	0.125	0.014
T7	0.120	0.034
T8	0.111	0.040

Table 7: Absorbed solar energy / electric energy input [Q_{sp}/Q_e].

performed by the Solver Tool from Microsoft Excel 2003 software, minimizing the root mean square error between the experimental values of moisture content of the tomatoes particles versus time and those calculated for the models. As shown in Table 6, the resulting R^2 values for three models were higher than 0.99, being slightly better the adjustments of Henderson and Pabis model.

Energy efficiency

The energy efficiency, defined as the ratio between absorbed solar energy (Q_{sp}), calculated with Eqn 7, and electric energy input (Q_e), fluctuated between 0.066 and 0.125, depending on the solar radiation level and also on the operating conditions (Table 7).

$$Q_{sp} = A_{col} \cdot cos(\alpha) \cdot \int_0^t I(t) \cdot dt \qquad (7)$$

Here, Q_{sp}, A_{col} and I are the heat provided by solar radiation [J/s], collector surface [m²] and radiation [W/m²], respectively. The alpha angle (α) corresponds to the tilt of the accumulator-panel (α=11°).

Even though these efficiency values are not very high, they result in energy saving and also in a reduction of CO_2 emission. These values could probably be improved by increasing the tomatoes load in the HSD, since in this work only 40% maximum capacity (15 kg) of the dryer was used.

Conclusions

The solar panel allowed increasing the air temperature (T_{sp}) up to 18°C above the ambient temperature, depending on the air flow rate and mainly of the solar radiation.

It was possible to obtain the drying curves at different operation conditions. The curves exhibited a good adjustment to the empirical models of Page, modified Page, and Henderson and Pabis, resulting in R^2 values higher than 0.99 for the three models, being slightly better the adjustments of Henderson and Pabis model.

The critical moisture content (Xc) was obtained indirectly from the drying curves. The statistical analysis showed that temperature and size had significant effects on Xc.

The sorption isotherms of rehydration were determined and adjusted with the Guggenheim-Anderson-Boer (GAB) and the Peleg models. Both models exhibited a good adjustment quality, with RMSE lower than 0.25.

The color parameters of dehydrated tomatoes indicate a notorious redness, in all runs. The final degree of water re-hydration was 80 ± 2% for all runs, in less than 20 minutes.

Finally, the solar energy input resulted in 6.6-12.5% energy saving. These values could even be improved by increasing the tomatoes load in the HSD.

Acknowledgment

The authors wish to thank the financial support of project FONDECYT Nº 1110101.

References

1. Farkas I (2004) Solar-drying of materials of biological origin, in Dehydration of Products of Biological Origin, Ed. By Arun Mujumdar, Science Pub Inc. 318-368.
2. Kadam D, Samuel DVK (2006) Convective flat-plate solar heat collector for cauliflower drying. Biosystems Engineering 93: 189-198.
3. Belessiotis V, Delyannis E (2011) Solar drying. Solar Energy 85: 1665-1691.
4. Santos BM, Queiroz MR, Borges TPF (2005) A solar collector design procedure for crop drying. Brazilian Journal of Chemical Engineering 22: 277-284.
5. Basunia MA, Abe T (2001) Thin layer solar drying characteristics of rough rice under natural convection. Journal of Food Engineering 47: 295-301.
6. Reyes A, Mahn A, Cubillos F, Huenulaf P (2013) Mushroom dehydration in a hybrid solar-dryer. Energy Conversion Management 70: 31-39.
7. Imre L, Palaniappan C (1996) Development of solar Drying. Drying Technology 14: 1381-1388.
8. Dufour P (2006) Control Engineering in Drying Technologies: Review and Trends. Drying Technology 24: 889-904.
9. Boughali S, Benmoussa H, Bouchekima B, Mennouche D, Bouguettaia H, et al. (2009) Crop drying by indirect active hybrid-solar-electrical dryer in the eastern Algerian Septentrional Sahrta. Solar Energy 83: 2223-2232.
10. El-Sebaii AA, Shalaby SM (2013) Experimental investigation of an indirect-mode forced convection solar dryer for drying thymus and mint. Energy Conversion and Management 74: 109-116.
11. Badescu V (2006) Optimum fin geometry in flat plate solar collector systems. Energy Conversion and Management 47: 2397-2413.
12. Karim MA, Hawlader MNA (2004) Development of solar air collectors for drying applications. Energy Conversión and Management 45: 329-344.
13. Tsamparlis M (1990) Solar drying for real applications. Drying Technology 8: 261-285.
14. Bhattacharya SC, Ruangrungchaikul T, Pham HL (2000) Design and Performance of a Hybrid Solar/Biomass Energy Powered for fruits and Vegetables. Proceedings of the World Renewable Energy Congress VI1161-1164.
15. Abdullah K (2009) Dissemination of Hybrid ICDC Solar Drying Systems, Renewable Energy & Sustainable Development in Indonesia: Past Experience-Future Challenges, Jakarta 19-20.
16. Palaniappan C (2009) Perspectives of solar food processing in India. International Solar Food Processing Conference.
17. Pangavhane DR, Sawhney RL (2002) Review of research and development work on solar dryers for grape drying. Energy Conversion and Management 43: 45-61.
18. Bennamoun L, Belhamri A (2003) Design and simulation of a solar dryer for agriculture products. Journal of Food Engineering 59: 259-266.
19. Triebe K (2009) Practical Application of Solar Tunnel dryers. International Solar Food Processing Conference.
20. Joshi CB, Gewali MB, Bhandari RC (2004) Performance of Solar Drying Systems: A Case Study of Nepal. IE(I) Journal-ID 85: 53-57.
21. Moradi M, Zomorodian A (2009) Thin layer solar drying of cuminum cyminum grains by means of solar cabinet dryer. American-Eurasian J Agric Enviromen Sci 5: 409-413.
22. Hassanain AA (2010) Unglazed Transpired Solar Dryers for Medicinal Plants. Drying Technology 28: 240-248.
23. Simate IN (2001) Simulation of the mixed-mode natural-convection solar drying of maize. Drying Technology 19: 1137-1155.
24. Vlachos NA, Karapantsios TD, Balouktsis AI, Chassapis D (2002) Design and testing of a new solar tray dryer. Drying Technology 20: 1243-1271.
25. Yaldyz O, Ertekyn C (2001) Thin layer solar drying of some vegetables. Drying Technology 19: 583-597.
26. Crank J (1975) The Mathematics of Diffusion, Oxford University Press: London.
27. Doymaz I (2004) Convective air drying characteristics of thin layer carrots. J Food Eng 61: 359-364.
28. Wang Z, Sun J, Liao X, Chen F, Zhao G, et al. (2007) Mathematical modeling on hot air drying of thin layer apple pomace. Food Res Int 4: 39-46.
29. Brooks MS, Abou El-Hana NH, Ghatly AE (2008) Effects of Tomato Geometries and Air Temperature on the Drying Behavior of Plum Tomato. American Journal of Applied Sciences 5: 1369-1375.
30. Araya-Farias M, Ratti C (2009) Dehydration of Foods: General Concepts. In Advances in Food Dehydration, Ed. by Cristina Ratti. CRC Press, Taylor & Francis Group, Boca Raton, FL.
31. Prothon F, Ahrné L (2004) Application of the Guggenheim, Anderson and de Boer model to correlate water activity and moisture content during osmotic dehydration of apples. Journal of Food Engineering 61: 467-470.
32. Peleg M (1993) Assessment of a semi-empirical four parameter general model for sigmoid moisture sorption isotherms. Journal of Food Process Engineering 16: 21-37.
33. Gaware TJ, Sutar N, Thorat BN (2010) Drying of Tomato Using Different Methods: Comparison of Dehydration and Rehydration Kinetics. Drying Technology 28: 651-658.
34. Doymaz I (2007) Air-drying characteristics of tomatoes. Journal of Food Engineering 78: 1291-1297.
35. Hossain MA, Amer BMA, Gottschalk K (2008) Hybrid Solar Dryer for Quality Dried Tomato. Drying Technology 26: 1591-1601.
36. Kostoglou M, Chrysafis M, Andritsos N (2013) Modelling Tomato Dehydration in a Tunnel Dryer Using Geothermal Energy. Drying Technology 31: 5-15.
37. Kerkhofs NS, Lister CE, Savage GP (2005) Change in colour and antioxidant content of tomato cultivars following forced-air drying. Plant Foods Hum Nutr 60: 117-121.